Journal of Applied Polymer Science

Poly(ethylene terephthalate) Nanoparticles Prepared by CO_2 Laser Supersonic Atomization

Akihiro Suzuki, Yoshiaki Shima
Interdisciplinary Graduate School of Medicine and Engineering, University of Yamanashi, Kofu 400-8511, Japan
Correspondence to: A. Suzuki (E-mail: a-suzuki@yamanashi.ac.jp)

ABSTRACT: Poly(ethylene terephthalate) (PET) particles were prepared by the irradiation of PET fibers with a carbon dioxide (CO_2) laser while atomizing them at supersonic velocities. A supersonic jet was generated by blowing air into a vacuum chamber through a fiber injection orifice. The fibers are melted by laser heating and atomized by the supersonic jet at the outlet of the orifice. The PET particles produced by CO_2 laser supersonic atomization conducted at a laser power of 34 W and at a chamber pressure of 10 kPa have an average particle size of 0.619 μm, high circularity, and a smooth surface that is not roughened by laser ablation. The novel CO_2 laser supersonic atomization technique can be used to easily prepare polymeric nanoparticles of various thermoplastic polymers using only CO_2 laser irradiation without the need for solvents and additives. © 2014 Wiley Periodicals, Inc. J. Appl. Polym. Sci. **2014**, *131*, 40909.

KEYWORDS: manufacturing; morphology; nanoparticles; nanowires and nanocrystals; polyesters

Received 9 January 2014; accepted 21 April 2014
DOI: 10.1002/app.40909

INTRODUCTION

Polymeric particles have many applications in various fields such as electronics, photonics, medicine, and environmental technology. Techniques for the preparation of polymeric particles can be roughly classified into the dispersion of preformed polymers and the polymerization of monomers using classical polymerization; the former uses solvent evaporation, electrospraying, aerosol solvent extraction systems, and rapid expansion of supercritical solutions,[1–6] whereas the latter involves the direct polymerization of monomers using emulsion and suspension polymerization.[7–13]

Solvent evaporation was the first method developed to prepare polymeric particles from a preformed polymer and is the most widely used technique to prepare polymer nanoparticles. Electrospraying is also a simple and versatile technique for the production of polymeric particles. However, such techniques require the dispersion of preformed polymers in solution with excess solvent, and it is difficult to completely remove the residual solvent from the particles produced.

Emulsion polymerization is used widely to produce various polymeric particles. Conventional emulsion polymerization systems use varied quantities of surfactants that must be eliminated from the final product, but are difficult to completely remove.

Here, we propose a new approach for the production of nanofibers that involves irradiation of a fiber with a carbon dioxide (CO_2) laser while the fiber is drawn at supersonic velocities and have named this preparation method CO_2-laser supersonic drawing. The fiber is instantly melted by irradiation with the high-power laser beam in the cold supersonic jet. CO_2-laser supersonic drawing has already been applied to various polymers[14–19] and can also be used to easily prepare their nanofibers without additional processes or solvents.

Recently, we have discovered that polymeric particles can be produced by irradiation of the fiber with the high-power laser while performing CO_2-laser supersonic drawing. Thus, we propose this method as a new approach to the production of polymeric particles and have named this preparation method CO_2 laser supersonic atomization (CLSA). CLSA is excellent with respect to the safety of particles because the polymer particles can be produced without solvents and additives, and the preparation process has a wide applicability compared with other conventional techniques for the preparation of polymeric particles. In this article, we present the preparation of Poly(ethylene terephthalate) (PET) nanoparticles by CLSA.

EXPERIMENTAL

The PET fibers used in the present study were prepared from commercial-grade PET pellets using a laboratory melt spinning machine. The as-spun PET fibers had an average fiber diameter of 136 μm, a 7.3% degree of crystallinity, and were almost completely amorphous and isotropic.

The morphologies of the produced particles were investigated using scanning electron microscopy (SEM; JSM-5700, Jeol Ltd.)

at an accelerating voltage of 10 kV. Prior to SEM observation, the samples were coated with platinum using a sputter coater. The average particle size and size distribution were measured using an image analyzer (SMile View, Jeol Ltd.). The average particle size was determined from the diameters measured at 100 different locations in the collected particle samples.

The melting of fibers by the heating laser during the supersonic atomization process was recorded with a high-speed camera (Motion Analysis Microscope VW-6000, Keyence) equipped with a long range zoom lens (VH-Z50L/W, Keyence). The high-speed camera is capable of high-speed recording up to 24,000 fps and the zoom lens has an 85 mm viewing distance at a maximum ×500 magnification.

Wide-angle X-ray diffraction (WAXD) patterns of the fibers were obtained using an imaging-plate (IP) film and an IP detector (R-AXIS DS3C, Rigaku Co., Japan). The IP film was attached to an X-ray generator (Rigaku Co.) using Ni-filtered Cu K_α radiation and operated at 40 kV and 200 mA. The sample-to-film distance was 40 mm. The fiber was exposed to the X-ray beam for 60 min from a 0.4 mm diameter pinhole collimator.

Differential scanning calorimetry (DSC) measurements were conducted using a calorimeter (Thermo Plus 2 DSC 8230C, Rigaku Co.) within the temperature range from 25°C to 300°C at a heating rate of 10°C min^{-1}. All DSC experiments were performed under nitrogen purge. The DSC instrument was calibrated using indium. The degree of crystallinity (X_c) was determined from the heat of fusion (ΔH_m) and the enthalpy of cold crystallization (ΔH_{cc}) using the following expression:

$$X_c = \frac{\Delta H_m + \Delta H_{cc}}{-126.6} \times 100, \quad (1)$$

where -126.6 J g^{-1} is used as the heat of fusion for the crystalline phase of PET.[20]

Figure 1 shows the apparatus used for CLSA, which consists of a spool to supply the fiber, a continuous-wave CO_2 laser with an output wavelength of 10.6 μm and a maximum power of 40 W, an acrylic vacuum chamber with Zn–Se windows and a 0.5 mm diameter fiber injection orifice for injecting the fiber, a power meter, a movable platen, a vacuum pump, and a high-speed camera equipped with the long-range zoom lens. The vacuum chamber was placed on the movable platen, which consists of a micro-alignment stage, a laboratory jack, and a turntable that can be moved parallel to the *Y* and *Z* axes, and can also be rotated about the laser irradiation point on the fiber, which allows fine adjustments to be made.

The velocity distribution of the air jet from the orifice was estimated by fluid analysis using a three-dimensional (3D) finite element method with ANSYS® CFZ 11.0 software. The analyses were estimated based on variation of the pressure.

RESULTS AND DISCUSSION

The as-spun PET fiber was drawn by the laser irradiation, so that nanofibers with various fiber diameters were obtained by varying the laser power and the chamber pressure. However, when the annealed PET fiber was drawn by laser irradiation at the same laser irradiation condition, polymer particles were obtained without nanofibers. The morphology of the polymer obtained by laser irradiation differed according to whether the as-spun fiber was annealed or not.

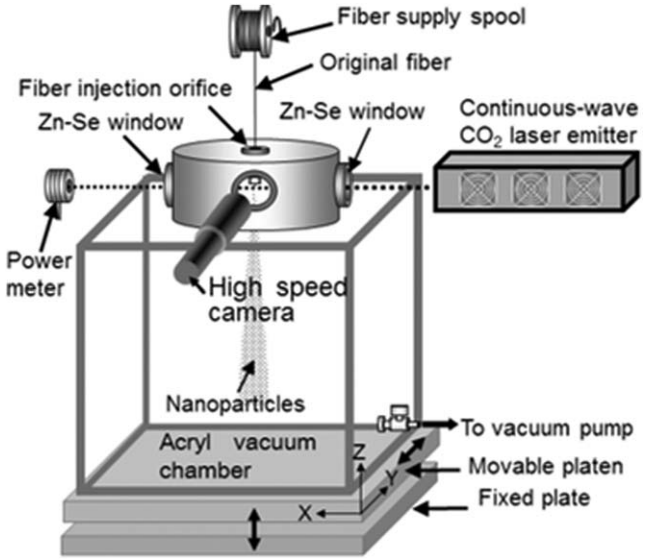

Figure 1. Schematic diagram of apparatus used for the CLSA process.

Figure 2 shows WAXD patterns of (a) the as-spun fiber and (b) the annealed fiber, and optical micrographs (×500 magnification) showing the laser irradiation points for (e) the as-spun fiber and (f) the annealed fiber under laser irradiation at $p_{ch} = 10$ kPa and at a laser power of 34 W. SEM micrographs of (g) the nanofiber and (h) the particle produced, and schematic diagrams for the formation processes of (i) the nanofiber and (j) the particle produced by laser irradiation of the as-spun PET fiber and the annealed fiber in the cold supersonic jet are also shown. The optical micrographs of the laser irradiation points were taken perpendicular to the laser beam using the high-speed camera equipped with the long-range zoom lens. The fiber was irradiated from a laser located to the left of the point in the micrograph. The as-spun fiber had a 7.3% degree of crystallinity and was almost completely amorphous and isotropic, as shown in Figure 2(a). The as-spun fiber with the lower degree of crystallinity does not have an effective physical network structure to interrupt plastic deformation, because no crystallites are present to act as cross-linking points [Figure 2(c)].

Annealing of the as-spun fiber was conducted at 260°C for 10 min at a constant length before laser irradiation. The annealed PET fiber had a 41% degree of crystallinity and was isotropic, as indicated by the WAXD pattern in Figure 2(b). The annealed fiber seems to be constructed of a physical network structure formed by crystallites that act as cross-linking points, as shown in Figure 2(d).

Laser irradiation of the as-spun fiber resulted in the formation of necking at the melt position, and a nanofiber was produced, as shown in Figure 2(e,g). Plastic deformation occurred rapidly when the drag force became larger than the intermolecular chain force [Figure 2(i)]. The molecular chains were highly oriented to the fiber axis without relaxation during rapid heating and cooling in the cold supersonic jet. The plastic deformation rate of the ultra-drawn fiber in the cold supersonic jet cannot

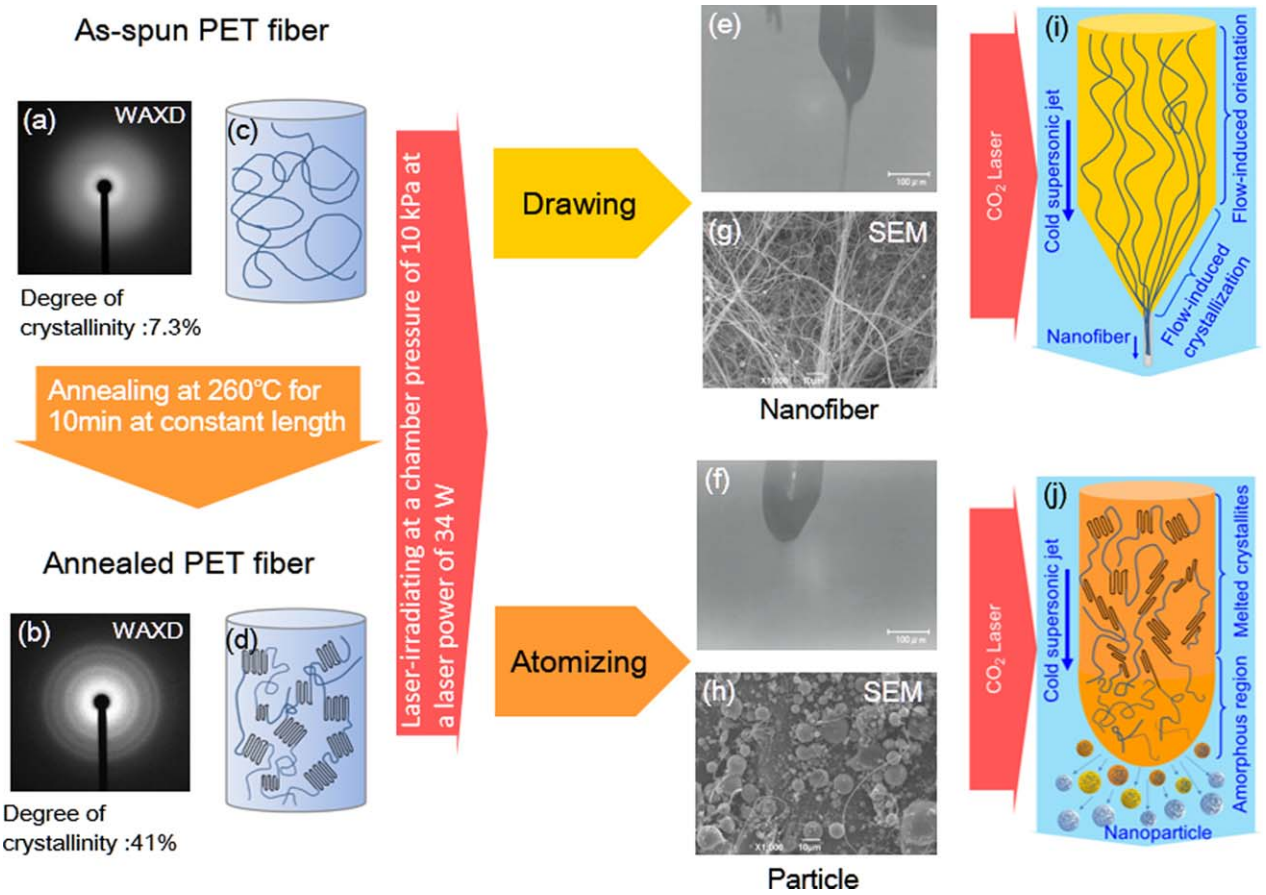

Figure 2. WAXD patterns of (a) the as-spun fiber and (b) the annealed fiber, and schematic diagrams of superstructure for (c) the as-spun fiber and (d) the annealed fiber. Optical micrographs (magnification ×500) showing the laser irradiation points for (e) the as-spun fiber and (f) the annealed fiber under the laser irradiation at $p_{ch} = 10$ kPa and at a laser power of 34 W. SEM micrographs of (g) the nanofiber and (h) the particle produced, and schematic diagrams for the formation processes of (i) the nanofiber and (j) the particle produced by laser irradiation of the as-spun PET fiber and the annealed fiber. [Color figure can be viewed in the online issue, which is available at wileyonlinelibrary.com.]

be measured directly; however, the drawing rate can be approximately estimated by assuming that the volume of fiber is constant during CO_2-laser supersonic drawing, as discussed later.

When the volumes before and after drawing are assumed to be equal, the following equation applies:

$$\left(\frac{d_0}{2}\right)^2 \pi L = \left(\frac{d_{av}}{2}\right)^2 \pi \ell, \tag{2}$$

where d_0 and d_{av} are the diameters of the original fiber and the drawn fiber, respectively, and L and $\ell$are the length of the original fiber and the drawn fiber, respectively. In eq. (2), L and ℓ are differentiated with respect to the time, and the following equation is obtained:

$$d_0^2 \frac{dL}{dt} = d_{av}^2 \frac{d\ell}{dt}, \tag{3}$$

where dL/dt and $d\ell/dt$ are the fiber supply rate (S_S) and drawing rate (S_D). Thus, eq. (3) can be rewritten as:

$$S_D = \left(\frac{d_0}{d_{av}}\right)^2 S_S. \tag{4}$$

The drawing rate can be calculated easily using eq. (4). The estimated drawing rate of the thinnest nanofiber ($d_{av} = 0.337$ μm) supplied at $S_S = 0.10$ m min^{-1} reached 486 m s^{-1}. Thus, extremely large plastic deformation occurs at supersonic speed during CO_2-laser supersonic drawing process. The as-spun fiber was ultra-drawn at supersonic drawing speed, which resulted in the production of a nanofiber.

However, the melting behavior of the annealed fiber is significantly different from that of the as-spun fiber, and the shape formed at the melting position is not typical necking, but a spherical shape, as shown in Figure 2(f). The product obtained by laser irradiation of the annealed fiber was, therefore, not a nanofiber, but a spherical particle, as shown in Figure 2(h). When the annealed fiber is laser-irradiated, the physical network built by the crystallites inhibits plastic deformation until the crystallites are melted. As the crystallites are melted, the physical network that inhibits large plastic deformation is simultaneously broken. The viscosity of the laser-irradiated fiber decreases rapidly by the rupture of the physical network, and the molten fiber becomes amorphous and is atomized by the supersonic jet. The completely melted fiber is atomized and becomes spherical, and the atomized particle is then quenched by the cold supersonic jet, which sets the shape to spherical, as shown in Figure 2(j).

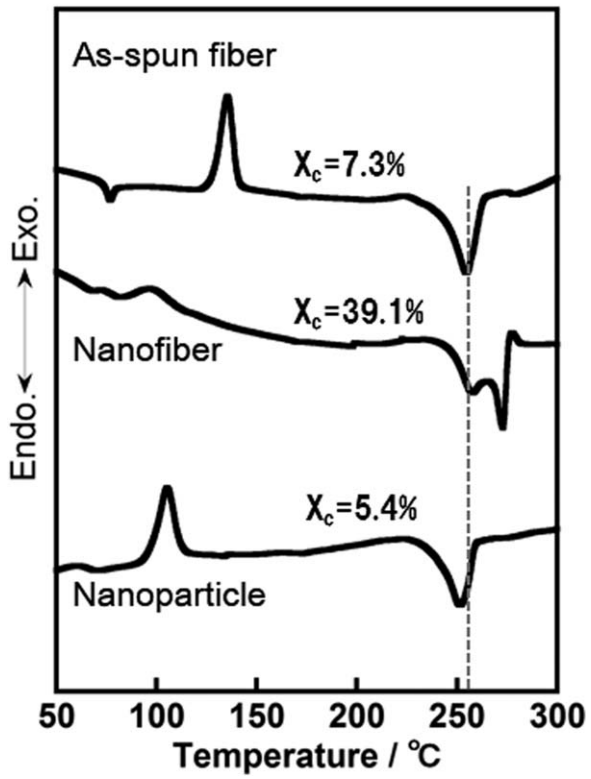

Figure 3. DSC curves for the as-spun fiber, the nanofiber, and the nanoparticle including the degree of crystallinity (X_c).

In laser-irradiating the as-spun fiber, when its viscosity reaches the viscosity capable of plastic deformation, the plastic deformation begins because the physical network that inhibits the plastic deformation does not exist, as shown in Figure 2(i).

The different melting behaviors of the two fibers at the melting position is attributed to whether the physical network is formed by crystallites or not. Therefore, the formation of PET particles is determined by annealing of the as-spun PET fiber prior to laser heating.

Figure 3 shows DSC curves for the as-spun fiber, the nanofiber, and the nanoparticle including the degree of crystallinity (X_c). The as-spun fiber exhibits a single exothermic peak at 135°C due to cold crystallization and a broad endothermic melting peak at 253°C, and has a 7.3% degree of crystallinity. The melting peak can be ascribed to lamellar crystals that form during the DSC measurement. The nanofiber was produced by laser irradiation of the as-spun fiber at $p_{ch} = 10$ kPa and $P_L = 34$ W. The nanofiber has two melting peaks at 258°C and 273°C. The lower melting peak is 5°C higher than that of the as-spun fiber, and the higher melting peak is 15°C higher than the lower melting peak. The higher melting peak is caused by an increase in the degree of perfection of the crystallites; X_c for the nanofiber is 39.1%, which suggests that flow-induced crystallization occurs during the drawing process in the supersonic jet.

Nanoparticles were produced by laser irradiation of a fiber that was annealed at 260°C for 10 min. The annealed fiber was

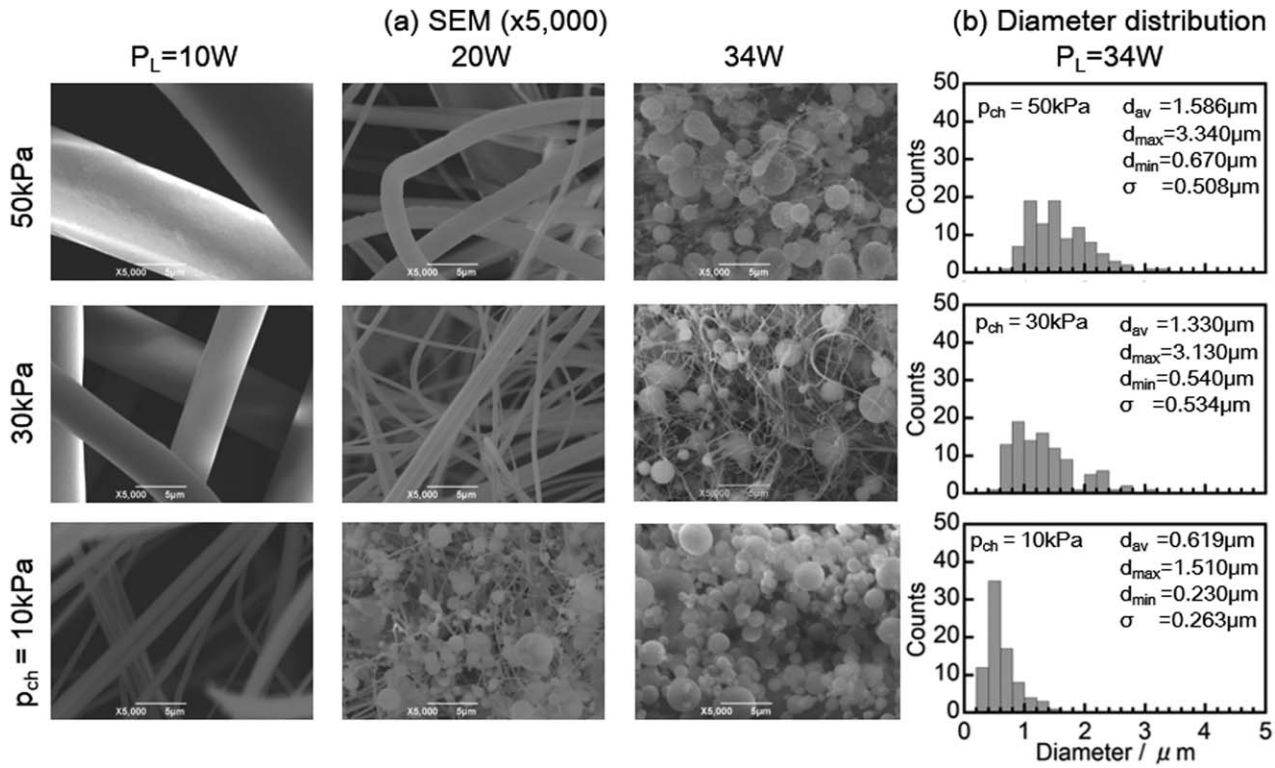

Figure 4. (a) SEM micrographs (magnification ×5000) of particles and fibers obtained at various laser powers (P_L) and chamber pressures (p_{ch}). (b) Particle size distributions, average particle size (d_{av}), maximum particle size (d_{max}), minimum particle size (d_{min}), and standard deviation (σ) for particles produced at $P_L = 34$ W and at three different chamber pressures.

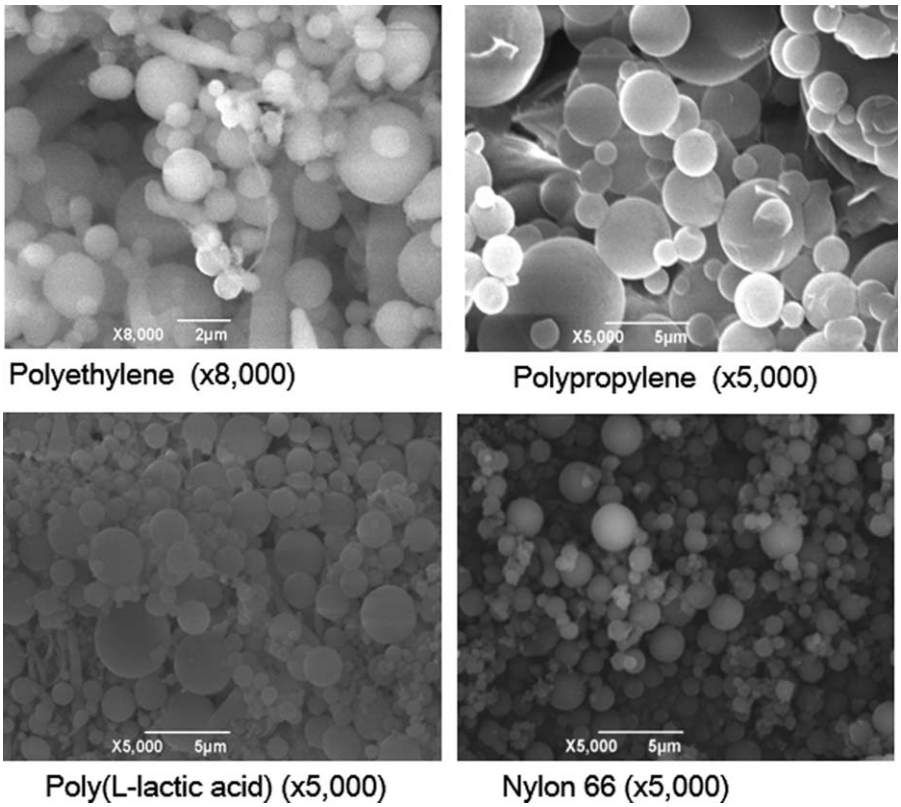

Figure 5. SEM micrographs of polyethylene, isotactic polypropylene, poly(L-lactic acid), and nylon 66 particles produced using the CLSA process.

laser-irradiated under the same laser irradiation conditions as those used to produce the nanofiber, i.e., at p_{ch} =10 kPa and P_L =34 W. The DSC profile for the nanoparticle has a single exothermic peak at 103°C due to cold crystallization and a broad endothermic melting peak at 252°C. The cold crystallization temperature (T_{cc}) is 30°C lower than that of the as-spun fiber, the shift of which is caused by an increase in the degree of orientation of the amorphous chains and by crystal seeds formed during CLSA. X_c for the particle is 5.7%, which is lower than that of the as-spun fiber and indicates that the nanoparticle obtained is amorphous. The production of spherical amorphous nanoparticles suggests that the atomized fiber was heated quickly by laser irradiation and then rapidly quenched in the cold supersonic jet.

Figure 4 shows (a) SEM micrographs (×5000 magnification) of particles and fibers obtained by laser irradiation of the annealed fiber at various laser powers (P_L) and chamber pressures (p_{ch}), and (b) particle size distributions together with average particle size (d_{av}), maximum particle size (d_{max}), minimum particle size (d_{min}), and standard deviation (σ) for the particles produced at P_L = 34 W and at three different chamber pressures. For CLSA conducted at P_L = 10 W, microfibers without particles were obtained at all chamber pressures, and the fiber diameter decreased with the chamber pressure. At P_L = 20 W, both microfiber and nanofiber were obtained at p_{ch} = 30 and 50 kPa, and a mixture of particles and nanofibers was produced at p_{ch} = 10 kPa. At P_L = 34 W, a mixture of particles and nanofibers was produced at p_{ch} =30 and 50 kPa, whereas particles without fibers were obtained only at p_{ch} = 10 kPa. The particles obtained by CLSA have high circularity, which is defined as the difference in the diameter between a circumscribed circle and an inscribed circle of the particle, and smooth surfaces that have not been roughened by laser ablation. The particle size decreases with the chamber pressure, and the particle size distribution gradually becomes narrower. The particles produced at p_{ch} = 10 kPa have d_{av} = 0.619 μm and σ = 0.263 μm, and no fibers were formed. The particles were obtained only for irradiation of the annealed fiber with higher laser power at lower chamber pressure.

PET nanoparticles were obtained by atomizing fibers melted by a CO_2 laser in a cold supersonic jet. The CLSA process can be used to produce particles of various polymers, such as polyethylene, isotactic polypropylene, poly(L-lactic acid), and nylon 66, as shown in Figure 5.

CONCLUSION

The spherical particles can be obtained only by the direct polymerization of monomers using emulsion and suspension polymerization, but the particles obtained contain solvents and additives. The polymer particles without solvents and additives can be produced by using a crusher, but the spherical particles cannot be obtained. On the other hand, the particle produced by CLSA is the spherical particles without any solvents and additives. CLSA can be used to easily prepare various nanoparticles of all types of thermoplastic polymers using CO_2 laser irradiation without the need for solvents and additives, or additional purification processes. Therefore, CLSA is considered to

be a "green" process for the production of polymeric nanoparticles. The polymeric particles obtained using CLSA have high circularity and smooth surfaces.

REFERENCES

1. Choi, S.; Lee, K.; Kwon, S.; Kim, H.; Choi, S.; Lee, K.; Kwon, S.; Kim, H. *J. Supercritical Fluid* **2006**, *37*, 287.
2. Barron, M. K.; Young, T. J.; Johnston, K. P.; Williams, R. O. *AAPS Pharm. Sci. Tech.* **2003**, *4*, 1.
3. Konan, Y. N.; Gurny, R.; Allémann, E. *Int. J. Pharm.* **2002**, *233*, 239.
4. Shiho, H.; Desimone, J. M. *J. Polym. Sci. Part A: Polym. Chem.* **1999**, *37*, 2429.
5. Wu, Y.; Kennedy, S. J.; Clark, R. L. *J. Biomed. Mater. Res. Part B: Appl. Biomater.* **2009**, *90B*, 381.
6. Jarmer, D. J.; Lengsfeld, C. S.; Randolph, T. W. *J. Supercritical Fluid* **2003**, *27*, 317.
7. Tseng, C. M.; Lu, Y. Y.; El-Aasser, M. S.; Vanderhoff, J. W. *J. Polym. Sci. Part A: Polym. Chem. Ed.* **1986**, *24*, 2995.
8. Takahashi, K.; Miyamori, S.; Uyama, H.; Kobayashi, S. *J. Polym. Sci. Part A: Polym. Chem.* **1996**, *34*, 175.
9. Kagawa, Y.; Minami, H.; Okubo, M.; Zhou, J. *Polymer* **2005**, *46*, 1045.
10. Musyanovych, A.; Schmitz-Wienke, J.; Mailander, V.; Walther, P.; Landfester, K. *Macromol. Biosci.* **2008**, *8*, 127.
11. Tiarks, F.; Landfester, K.; Antonietti, M. *J. Polym. Sci. Part A: Polym. Chem.* **2001**, *39*, 2520.
12. Raoa, J. P.; Geckeler, K. E. *Prog. Polym. Sci.* **2011**, *36*, 887.
13. Landfester, K. *Adv. Mater.* **2001**, *13*, 765.
14. Suzuki, A.; Aoki, K. *Eur. Polym. J.* **2008**, *44*, 2499.
15. A.; Tanizawa K. *Polymer* **2009**, *50*, 913.
16. Suzuki, A.; Yamada, Y. *J. Appl. Polym. Sci.* **2010**, *116*, 1913.
17. Suzuki, A.; Shimizu, R. *J. Appl. Polym. Sci.* **2011**, *121*, 3078.
18. Suzuki, A.; Arino, K. *Eur. Polym. J.* **2012**, *48*, 1169.
19. Suzuki, A.; Hayashi, H. *Exp. Polym. Lett.* **2013**, *7*, 519.
20. Brandrup, J.; Immergut, E. H., Eds. Polymer Handbook, 4th ed.; John Wiley & Sons: New York, **1998**; pp. VI, 42.